Optical Links for the ITK

Todd Huffman[a], Tobias Flick[b],Tony Weidberg[a] and Jingbo Ye[c]

[a] *Physics Department, Oxford University, UK.*

[b] *Fachbereich C, Physik, University of Wupertal, Germany.*

[c] *Physics Department, Southern Methodist University, UK.*

Abstract

This document describes the proposed optical links to be used for the ITK in the phase II upgrade. The current R&D for optical links pursued in the Versatile Link group is reviewed. In particular the results demonstrating the radiation tolerance of all the on-detector components are documented. The bandwidth requirements and the resulting numerology are given.

ATL-UPGRADE-PUB-2013-005
14/02/2013

Contents

1. Introduction and Motivation

In the current generation of LHC experiments, different optical links have been developed for the 4 experiments. Even within ATLAS, there is a wide diversity of systems used for the various sub-systems, as well as differences between data and TTC links for the same sub-system. There have been problems with several of the optical links used in ATLAS[1] particularly with those based on non-commercial systems. For the upgrade it would therefore be better to put more resources into developing one common and very reliable system. This is of particular concern for the ITK as access to the on-detector optoelectronics once the detector is installed, will either be impossible, or at best extremely difficult. The use of optoelectronic components in the ITK impose some constraints that are not relevant for commercial components:

1. All components must be sufficiently radiation tolerant to withstand the fluences and ionizing doses corresponding to an accumulated luminosity of 3000 fb^{-1}.
2. The system must be sufficiently robust in the presence of Single Event Upsets (SEU) caused by the radiation field.
3. The components must be as low mass as possible and used preferentially low Z material.
4. Magnetic materials should be avoided.

There are common challenges faced by ATLAS and CMS for the optical links. Therefore for HL-LHC, groups from ATLAS and CMS are collaborating on a joint project to develop a Versatile Link (VL) which could be used in all the sub-systems required for ATLAS. Another advantage of this common approach is that it will minimise the development cost, compared to that of developing many solutions. This is very important because although the full costs of the development stages are hard to quantify, they are significant compared to the production costs.

The strategy adopted by the VL project is to make minimal modifications to existing commercial components, thus benefiting from the extensive reliability testing of large scale manufacturers as well as the extent to which these components are “qualified by the customer”. Such a strategy has been successfully adopted by CMS for their existing optical links. For the backend system, there are no additional constraints, so fully commercial components should be used.

2. Bandwidth Requirements

2.1 Strip Detector

The output data rate from the HCC is 160 Mbits/s. For the barrel short strips with a half-length of 1.2 m there would be 12 modules per side. Allowing for two hybrids and HCC per module, the resulting data rate at the End of Substructure (EoS) would be 3.84 Gbits/s. Note that for the case of the RoI track trigger, there would be no additional bandwidth requirements and the trigger information would be interleaved with the normal data readout. The self-seeded track trigger would require additional bandwidth but the requirements have not yet been evaluated. The data rates required for the TTC links are lower but it will be convenient to use the same speed for the TTC links as for the data links. The current straw-man layout for the strip detector requires 1672 bi-directional links. If similar fibre cables are used as in the current SCT and Pixel detectors (which contain up to 96 fibres), this would require about 20 fibre cables of diameter 10.5 mm. If it was decided to use full redundancy for the optical links, this would require doubling the number of optical links.

2.2 Pixel Detector

The requirements for the data readout of the pixel system are based on the assumption that the full data would be readout at the L0 rate of 500 kHz. The requirements for the TTC system would be identical to that of the strips.

3. System Aspects

The VL is based on bi-directional optical links. The increased number of channels and hit occupancy for the ITK compared to the existing tracker will require an order of magnitude higher total bandwidth. It is not feasible from the cost or material point of view to increase the number of optical links, therefore the bandwidth of each link should be greatly increased from the very low values used in the existing SCT & Pixel detectors (40 to 80Mbits/s). The most economical strategy is to use the highest practical bandwidth. This is limited not by the fibres but by the speed of custom radiation hard electronics. The VL being developed is based on the SFP+ standard which operates at a speed of 4.8 Gbits/s so there should be fewer links required for the ITK than the existing ATLAS tracker. There are several advantages and disadvantages of operating at 850 nm (multi-mode) compared to 1310 nm (single-mode) which will be explained in this note. Therefore the VL project is developing systems for both wavelengths. Which version will eventually be used by ATLAS will be decided before the production phase, based on performance and cost considerations. The VL is planned to be used in conjunction with the GBT[3] as illustrated in Figure 1.

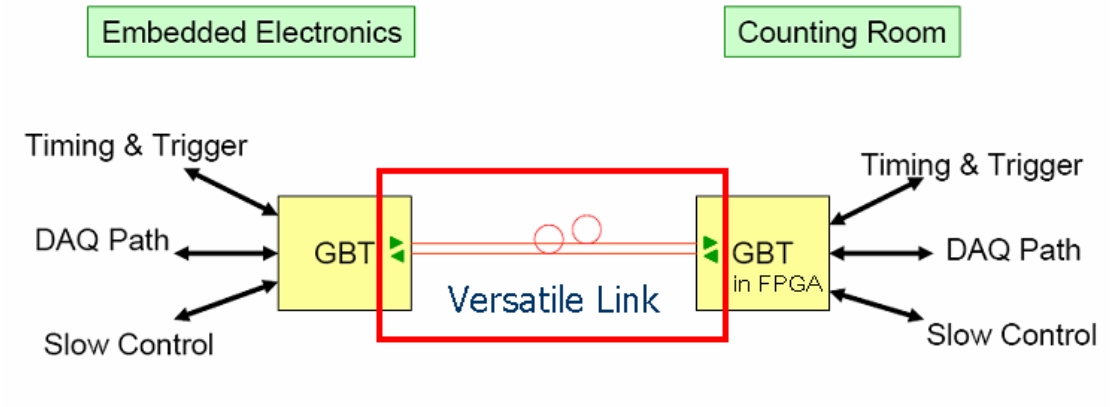

Figure 1 GBT and VL system

For the data links the GBT acts as a multiplexer taking data from several modules and creating a high speed serial signal. Environmental monitoring data can also be fed into the data stream through the GBT. The serial data stream communicates with a custom radiation tolerant laser driver ASIC (GBLD[5]) which send the data over fibre via a laser. The laser could be a VCSEL for the 850 nm option or an Edge Emitting Laser (EEL) for 1310 nm. However if suitable VCSELs are developed in industry for SM operation at 1310 nm then this could be an attractive option. For the TTC links the optical signal is received by a photodiode and followed by a radiation tolerant Trans-Impedance Amplifier (TIA). For the TTC links The GBT acts as a de-multiplexer to send common TTC data to different modules.

The VL is protocol agnostic, apart from requiring DC balance. For the data links the GBT wraps the data packets (payload) into a header, adds data for error correction, and uses data scrambling to ensure DC balance. Data Scrambling is an attractive way of achieving DC balance as it requires no additional overhead in data rates (as opposed to other ways of achieving DC balance such as 8b10b). The use of data scrambling for ATLAS data was investigated in [4]. The current error correction scheme allows for 80 bits of payload for each 128 bits, thus providing 3.2 Gbits/s of useful data. This provides multi-bit error correction which is required for the TTC links which will have significant SEU rates in the *p-i-n* diodes. However a lighter error correction scheme could be used for the data links (for which no significant SEU rates are expected) to provide higher data rates (e.g. 3.84 Gbits/s as required for the short strips).

3.1 Link Architecture Options

The simplest architecture for the optical links is Point to Point. However the VL is compatible with more sophisticated architectures used in Passive Optical Netowrks (PONs) as shown in Figure 2. One variant of a PON that is being considered for application to the TTC links is the

use of optical couplers. This would allow the optical data from one TTC link to be split and sent to several VL receivers. This option has the advantage of reducing the number of channels of transmitters required in USA15 as well as reducing the number of fibres. Note that this option would require increasing the width of the address field in the GBT, which could be achieved in a second iteration of the chip.

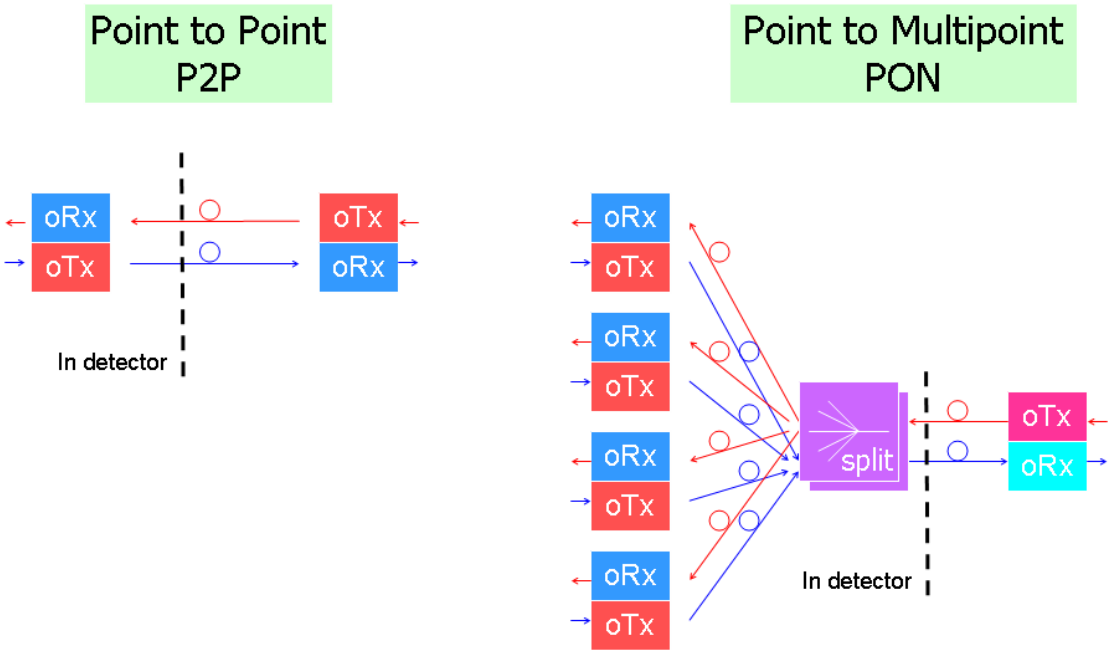

Figure 2 VL P2P and PON architecture. OTx (ORx) refers to optical transmitters and receivers. In the ITK, OTx and ORx will be combined into a transceiver, the VL TRx.

4. Versatile Link

The components required are broken down into on-detector components (section 4.1), passive components (section 4.2) and backend optoelectronics (section 4.3). For the first two classes of components, the radiation tolerance will be reviewed as well as the expected rate of SEUs. The VL power budget is given in section 4.4.

4.1 On-detector optoelectronics

The basic building block is the Versatile Tranceiver, VTRx, which consists of a transmitter (VTx) and receiver (VRx). The Tx consists of a laser driver custom radiation-hard ASIC (GBLD[5]) and the laser with an LC fibre connector. The Rx consists of a *p-i-n* diode coupled to an LC fibre connector and a Trans Impedance Amplifier (TIA). The package is based on the commercial SFP+, with the minimal set of modifications required to make it compatible with operation inside an LHC detector.

Firstly the ferrite bead used in the biasing circuit for the laser driver, is incompatible with operation in a magnetic field. This is therefore removed and the circuit redesigned. Secondly the two ASICs in the package are replaced with custom radiation hard ASICs, the GBT laser driver GLD and the GBT TIA. These ASICs are designed in the context of the GBT project and are described in another backup note [5]. We note that the GBLD is being specifically designed to be compatible with either VCSELs or EELs. This implies that it can operate with low output drive currents required for the VCSELs as well as the higher currents required for EELs. The drive current can be adjusted to accommodate the expected increase in threshold current with radiation damage. The TIA includes a limiting amplifier, so that it provides a digital output.

The third change required for the VTRx package is to reduce the material budget. This is achieved by replacing the metal cage surrounding the components with a custom plastic part[8]. Tests will be performed on EMI and if necessary the plastic part could be extended and coated with a thin metal (copper) layer to provide electrical screening. This concept then keeps the same Optical Sub Assemblies (OSA) as used in the commercial SFP+ package, so that the reliability of the critical optical components should not be degraded. The first prototypes of the package have been produced using 3D printing.

A photo of a prototype package is shown in Figure 3.

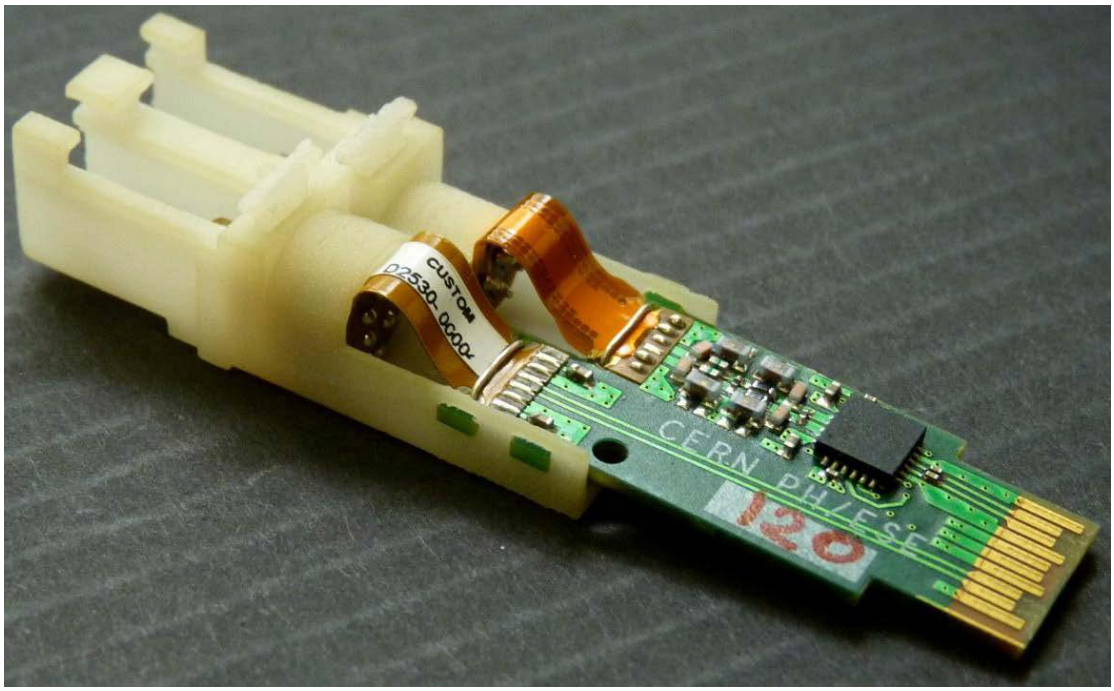

Figure 3 VTRx prototype showing the plastic part housing the OSAs and the LC fibre connector latches as well as the PCB with a laser driver. The TIA is integrated into the ROSA package in order to minimise stray capacitance.

The first prototypes confirmed basic functionality and developments of the plastic part will ensure that the required mechanical precision is achieved. Further work on the VTRx package is required to select a suitable radiation hard plastic, and to verify the properties under thermal cycling . First results of EMC/EMI tests showed no excess emission from the VTRx compared to a normal PCB. Tests of noise injection from a VTRx running asynchronously next to a prototype strip stavelet, showed no evidence for excess noise.

Prototype VTRxs have been produced for all flavours of VCSELs/EELs and commercial laser drivers/GLD[8]. Detailed performance measurements have been made and compared to the specifications. All flavours showed functionality but there were problems with the GBLD. A summary of the results of the tests of the GBLD/VCSEL variant is given in

Table 1. The fall time and deterministic jitter are slightly out of specification for the VTRx with GBLD but the VTRx with a commercial laser driver is fully compliant with all the specifications. Nevertheless the resulting eye diagram looks quite encouraging as shown in Figure 4 and Bit Error Rates (BER) lower than the specified value of 10^{-12} can be achieved. The remaining problems with the design are thought to be due to incorrect modeling of the parasitics. These problems are addressed in the new design GBLD-V4, which is expected to meet all the specifications. The GBLD-V4 was submitted for fabrication in November 2011.

Parameter	Normalization	4mA	5mA	6mA
OMA	OMA/300uW	1.96	2.27	2.55
Eye Height	Eye Height/(0.6*OMA)	1.09	1.26	1.35
ER	ER/3	1.54	1.91	2.25
1/Tr	(1/Tr)/(1/70ps)	1.10	1.18	1.63
1/Tf	(1/Tf)/(1/70ps)	0.92	0.90	0.87
1/Tj	(1/Tj)/(1/0.25UI)	1.21	1.26	1.18
1/Dj	(1/Dj)/(1/0.12UI)	0.93	0.97	0.90

Note: Bit rate = 4.8 Gb/s, UI = 208 ps

Table 1 Test results for the VTx with GBLD and VCSEL for different amplitudes of the drive current. OMA=optical modulation amplitude, Eye= vertical height of error free region at the centre of the eye diagram, ER=Extinction Ratio, Tr=rise time,Tf=fall time, Tj=total jitter, Dj=deterministic jitter. Values are normalised so that numbers above 1 exceed the specifications.

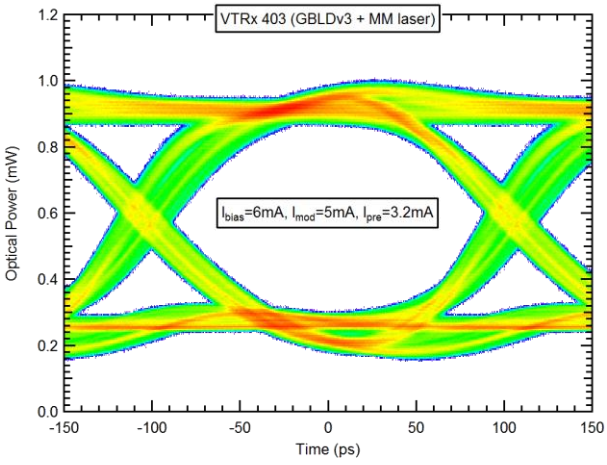

Figure 4 Eye diagram for the VTRx with GBLD and VCSEL operating at a data rate of 4.8 Gbits/s.

Further work on the VTRx package is required to select a suitable radiation hard plastic, to verify the properties under thermal cycling and to perform EMC/EMI tests.

4.1.1 Radiation Harness of Lasers

The ASICs are being fabricated in the IBM 130 nm process, so they are expected to be sufficiently radiation hard. An R&D programme to select suitably radiation hard lasers and *p-i-n* diodes has identified candidate devices. The lasers (both VCSELs and EELs) show significant annealing after radiation, therefore the effects of annealing need to be taken into account. The effect of radiation on these lasers results in an increase in threshold current and a decrease in slope efficiency. If the laser currents are increased too much to compensate for the increased threshold, the resulting junction temperature increase causes the optical output to decrease. This then results in curves of optical power versus current and voltage (LIV) to show maxima. This effect is illustrated for EELs[9] in Figure 5.The maximum optical power as a function of drive current can then be determined for a given fluence.

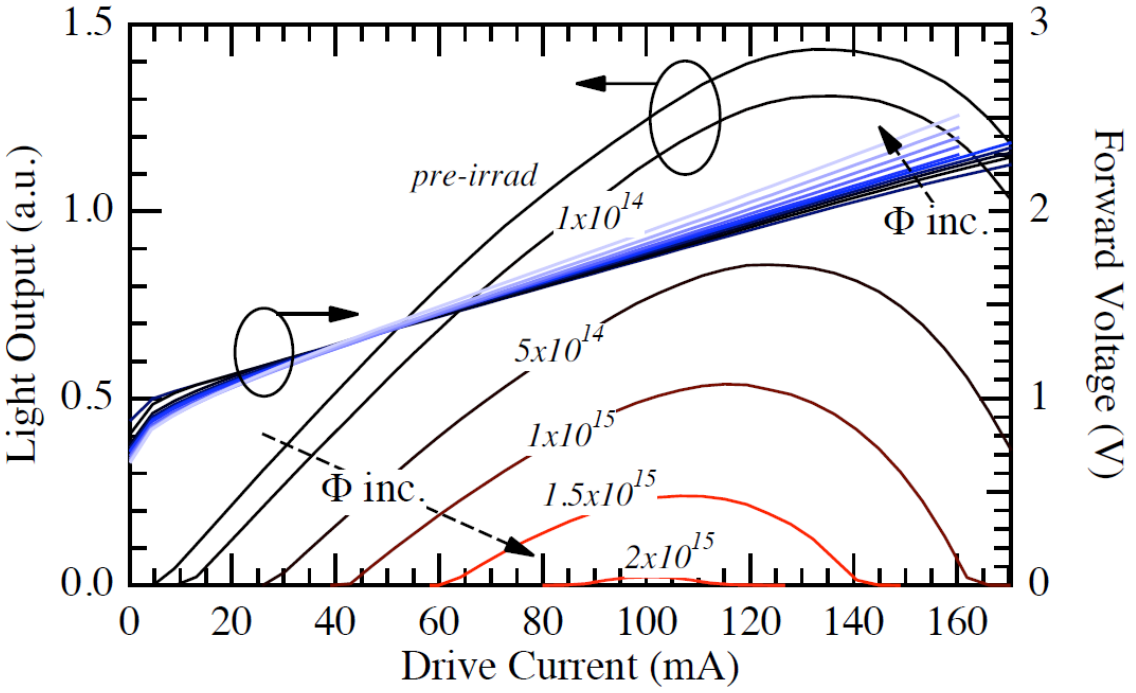

Figure 5 Light output and forward voltage versus drive current (LIV curves) for an EEL after several fluences of 20 MeV neutrons.

There is very significant annealing of the radiation damage for both EELs and VCSELs[9] as illustrated in Figure 6. VCSELs show less radiation damage than EELs.

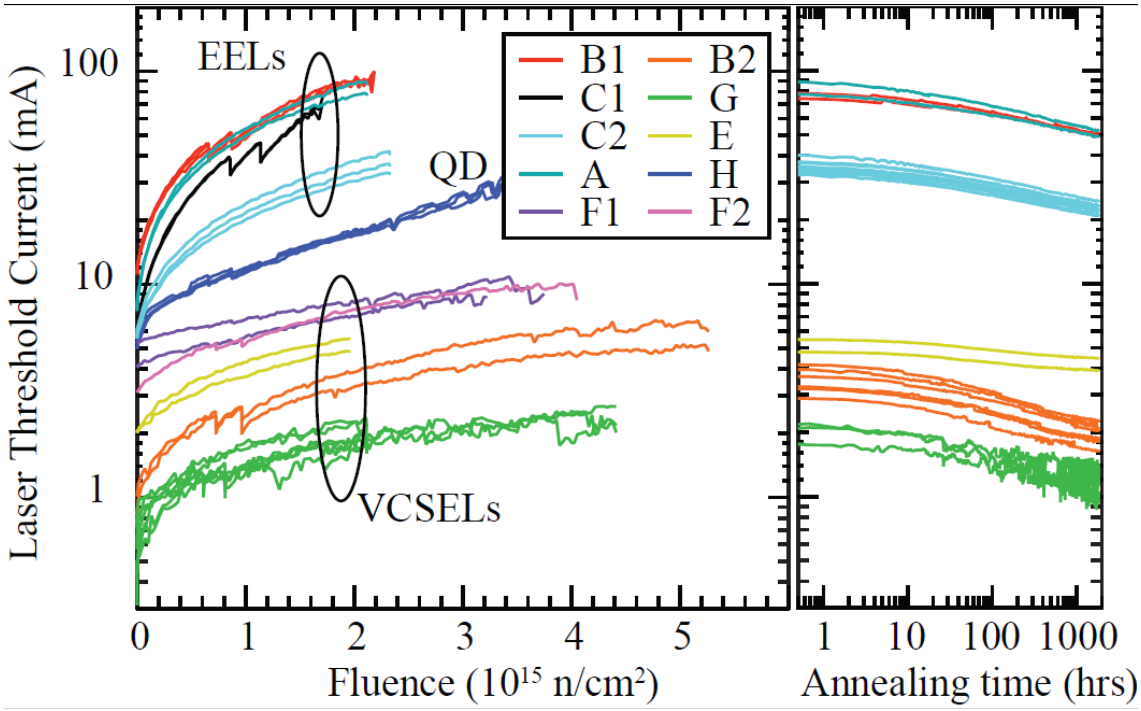

Figure 6 Laser threshold as function of 20 MeV neutron fluence (left) and post-radiation annealing time (right) for EELs, QD (quantum dot lasers) and VCSELs.

Since the fluxes used in these tests are inevitably many orders of magnitude higher than will be experienced by devices at HL-LHC, it is necessary to extrapolate these results to the lower fluxes. An annealing model has been developed and used to fit the data. Radiation tests have been performed with both 20 MeV neutrons and 191 MeV/c pions to determine empirical damage ratios. This annealing model can then be used to scale the measured increases in leakage current to the expected values at the lower fluxes expected at HL-LHC and the results are shown[9] in Figure 7.

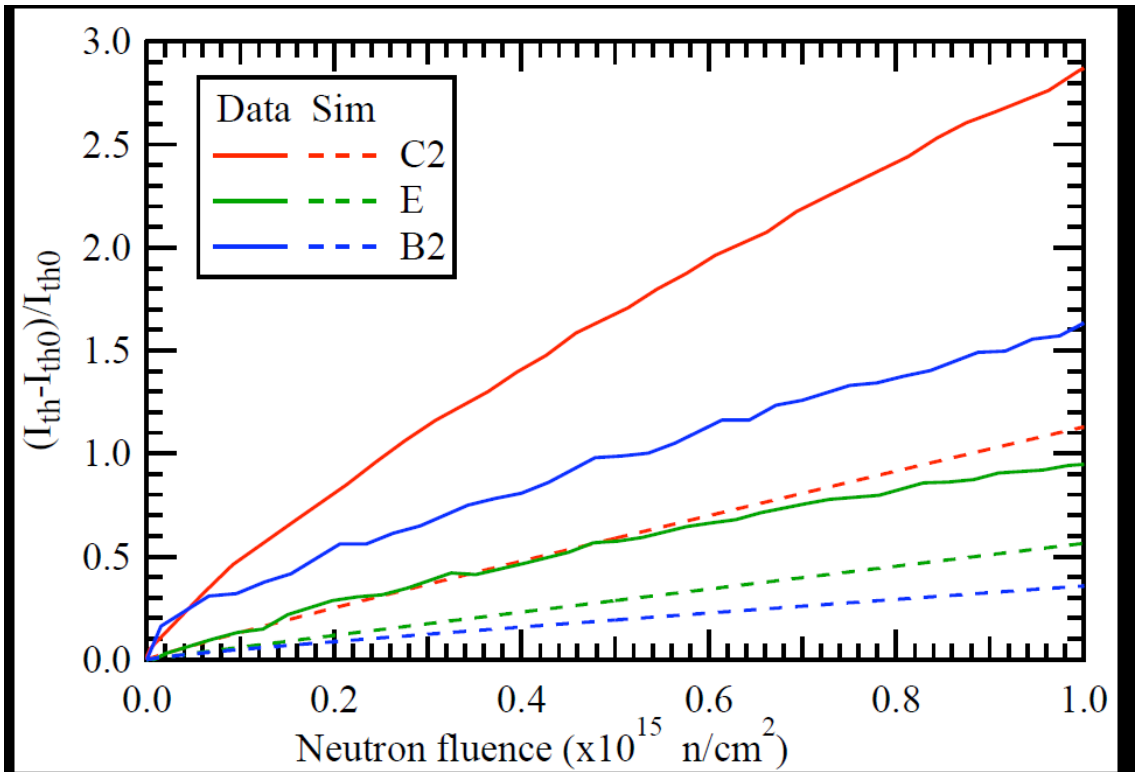

Figure 7 Fractional increase in laser threshold versus 20 MeV neutron fluence. The solid lines are the measured values at a flux of 1.5-3 10^{10} n $cm^{-2}s^{-1}$ and the dashed curves are the predictions of the annealing model to the lower flux expected at HL-LHC of 10^7 n/$cm^{-2}s^{-1}$. Device C2 is an EEL and E and B2 are VCSELs.

Radiation tests were performed with 20 MeV neutrons and 191 MeV/c pions to determine empirical damage factors. The measured values were similar to those expected from the Non Ionising Energy Loss (NIEL) hypothesis. These tests are based on DC measurements, therefore to understand the effects of radiation on AC performance, the Relative Intensity Noise (RIN) was measured before and after radiation. This showed no appreciable change in the laser resonance frequency[9]. Finally the annealing model can be used to predict the long term increase in leakage current expected at the HL-LHC allowing for an annual cycle of 8 months of operation and 4 months of annealing. The results for EELs[9] are shown in Figure 8.

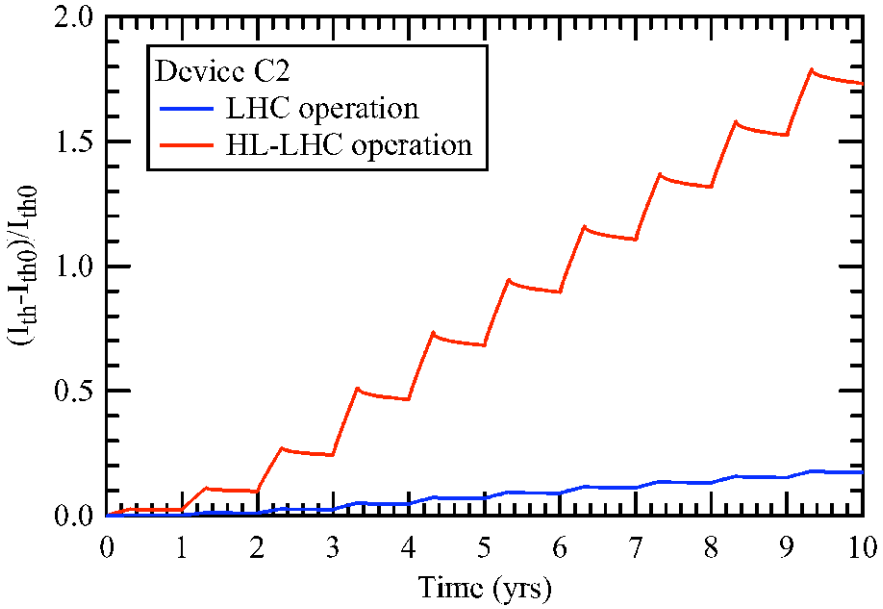

Figure 8 Predicted relative increase in threshold current as a function of time for an EEL at HL-LHC.

The effect of the increase in threshold current for an EEL can be mitigated by increasing the laser drive current by up to 20 mA. The GBLD is designed to have a programmable bias current up to 45 mA. Therefore we do not anticipate any decrease in peak optical power for EELs at HL-LHC. The increase in threshold current for VCSELs is much smaller. This implies that the advantage of the VCSELs over the EEL to be the lower power consumption, although this would be a small contribution to the total power budget of the ITK.

4.1.2 Radiation Hardness of *p-i-n* Didoes

The two effects of radiation damage on *p-i-n* diodes are an increase in leakage current and a decrease in responsivity. For GaAs devices there is no significant increase in leakage current, whereas the InGaAs devices show very significant increases as shown in Figure 9. However the TIA is designed to cope with the large leakage currents expected at the end of life and still maintain acceptable system performance. The changes in responsivity with fluence is larger for GaAs than InGaAs *p-i-n* diodes as shown in Figure 9. This shows clearly that the responsivity decrease is significantly smaller at the highest fluences for InGaAs than GaAs *p-i-n* diodes. Therefore InGaAs devices will be used in both flavours of VL (850 nm and 1310 nm). Since NIEL scaling is not established for InGaAs devices, tests have also been performed with neutron beams and empirical damage constants have been determined.

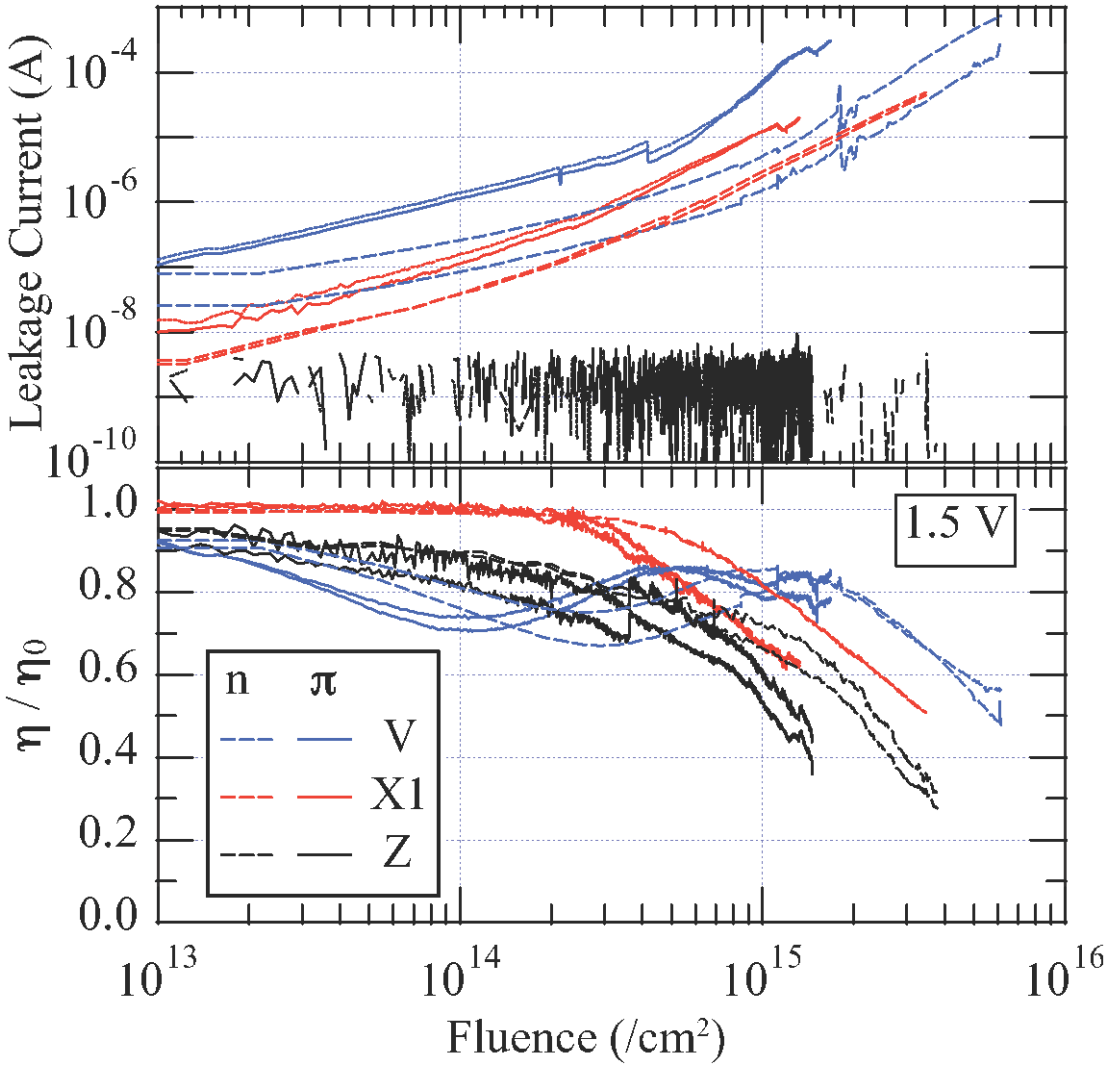

Figure 9 Leakage current (upper panel) and relative responsivity (lower panel) as a function of fluence for GaAs and InGaAs *p-i-n* diodes. Device Z is GaAs and V and X1 are InGaAs.

4.1.3 Single Event Upsets

In addition to total fluence effects, we also have to consider the SEU effects. SEU rates have been measured in pion test beams at PSI. As expected from previous studies significant SEU rates have been measured. For the first time, the effects of multiple bit errors have been studied in detail. Most but not all of the errors are due to 0s being mistaken for 1s. The error correction implemented in the GBT was demonstrated[10] to be very effective as illustrated in

Figure 10.The error correction can correct bursts of errors up to 16 bits long. Longer error bursts were observed when commercial ROSAs were used but with the GBT TIA these were not seen and the error correction was fully efficient at correcting for SEUs. Therefore this error correction scheme will be used for the TTC links.

A similar study was performed for the data links using the VTx and no evidence for SEUs was found. The GBTx use TMR to minimise sensitivity to SEU but the robustness of the GBTx still needs to be determined. If the SEU rates for the GBTx are sufficiently low the forward error correction (FEC) scheme would not be required for the data links (it will definitely be used for the TTC links to mitigate the expected SEUs in the on-detector p-i-n diodes). Therefore if we do not need the FEC, the data links could be operated in wide field mode, which would increase the useful data rate to 4.48 Gbps.

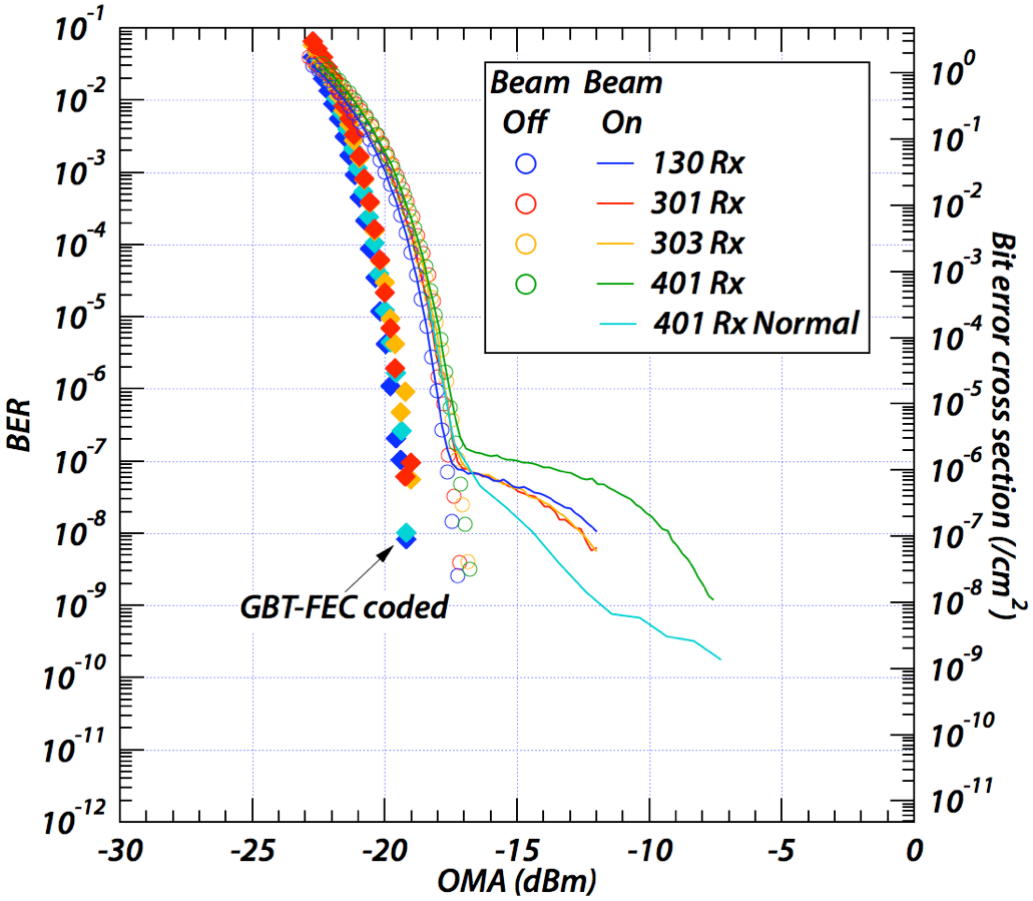

Figure 10 BER versus OMA for beam on and beam off data, with and without FEC.

4.2 Passive Components

The passive components required for P2P optical links consist of fibres, optical connectors and fibre cables and jackets. All these components must be sufficiently radiation hard for HL-LHC operation and the radiation tests that have been performed are reviewed in section 4.2.1 to 4.2.3. The PON architecture would also require optical couplers and the radiation tests for candidate devices is discussed in section 4.2.4.

4.2.1 Optical Fibres

Many commercial optical fibres are not sufficiently radiation hard for application in the HL-LHC environment. A necessary but not sufficient condition for a fibre to be radiation hard is that it does not contain any phosphorous in the core. Radiation hardness of fibres has been studied for many applications, including the current generation of LHC experiments. However the radiation hardness needs to be verified for the higher doses expected at HL-LHC. In the ITK, the fibres will be exposed to radiation at low temperatures, around T~ -25°C. Previous results in the literature (and confirmed by our tests) show that the effect of radiation damage on fibres at low temperature is greatly enhanced because the beneficial thermal annealing is suppressed.

The first test performed in the context of the VL studied the radiation hardness of candidate SM and MM optical fibres (under warm operating conditions) using ^{60}Co source at the SCK-CEN reactor and at BNL[11]. The tests used real time monitoring during the fibre radiation so that the Radiation Induced Attenuation (RIA) could be measured as a function of ionizing dose. The RIA versus time is shown in Figure 13. The fibre was removed from the radiation zone and returned to the radiation zone after about 31 hours of exposure. The fibre appears to show rapid annealing of the RIA after it is removed from the radiation zone. However after the fibre is returned to the radiation zone, it appears to remember the previous damage and the RIA quickly returns to the value it had before the fibre was removed. Therefore it is essential that all fibre testing be performed with active monitoring as before and after radiation (passive) testing would give over optimistic results. There is an initial spike in the RIA versus dose which then decreases to a lower value before starting to rise with further dose. The possible explanations of this effect are discussed in [11] but comparison with tests at lower dose rates show that this effect is an artifact of the very high dose used and will not be relevant for the very much lower dose rates expected at HL-LHC. The comparison of the data taken with different sources at different dose rates, are shown in Figure 13. The data clearly show that there is a very strong dose rate effect, with the lower dose rates corresponding to lower RIA values. Another test showed that there was also very strong optical annealing. With further studies it might be possible to understand these effects and build a model that we could use to

predict the RIA of the fibre as a function of dose. However we have chosen to use a simpler engineering approach;

- Use the ATLAS radiation maps (Figure 12) scaled to HL-LHC fluences, to give the expected dose along the fibre route.
- Perform fits to the fibre RIA data at different dose rates.
- Perform a piecewise integral along the fibre route to predict the total RIA, using the lowest dose rate data available.

This procedure gives a conservative upper limit to the expected RIA and showed that with warm fibre data it would be possible to qualify the Infinicor SX+ MM fibre as well as the Corning SMF-28 SM fibre.

The first attempts to determine the RIA at low temperatures to the full HL-LHC dose used a very high dose rate of 27 kGy(Si)/hour. The results were mixed but we were able to qualify the SM fibre from producer X[12]. The RIA in other fibres was so severe that the signals were outside the dynamic range of the photo-detector. Therefore the blow-off CO_2 system was adapted to be able to exchange CO_2 bottles and thus provide continuous cooling during an exposure lasting 10 days. The following fibres were studied in these exposures[13]: two SM fibres Corning-SMF-28e and Draka Elite SRH-MMF and two MM fibres, Corning Clearcurve OMA 4 and Draka Elite SRH-MMF. The two Draka fibres are custom fibres designed to be radiation tolerant but are available commercially. The Corning SMF-28e and the Corning Clearcruve OMA 4 are COTs components for which warm fibre radiation data had given encouraging results. The results showed much lower values of RIA at the dose rate of 0.66 kGy(Si)/hour compared to our previous data at 27 kGy(Si)/hour. Two of the four types of fibres showed a clear anti-correlation of RIA with temperature and this was corrected for as shown in Figure 14. The empirical fits were used to calculate the expected RIA in an ATLAS fibre route and the results are summarized in Table 2. All 5 fibres have an expected RIA< 1 dB. We note that these calculations give pessimistic worst case values as no corrections are made for long term annealing. Therefore all these fibres can be considered qualified for use in the ITK for temperatures above -30°C.

Table 2 Expected RIA for fibres from the ITK to USA15. The data from Producer X was taken at higher dose rates in 2010. For the Corning SMF-28e, separate data was used to evaluate the RIA inside the ITK (cold) and outside (warm). For the other fibres only the cold fibre RIA data was available. In addition no corrections for dose rate effects were made. Therefore these values should be considered as conservative upper limits.

Fibre	RIA (dB)
Corning SMF-28e (SM)	0.961
Draka Elite SRH-SMF (SM)	0.0643
Corning Clearcurve OM4 (MM)	0.580
Draka Elite SRH-MMF (MM)	0.143
Producer X (SM)	0.277

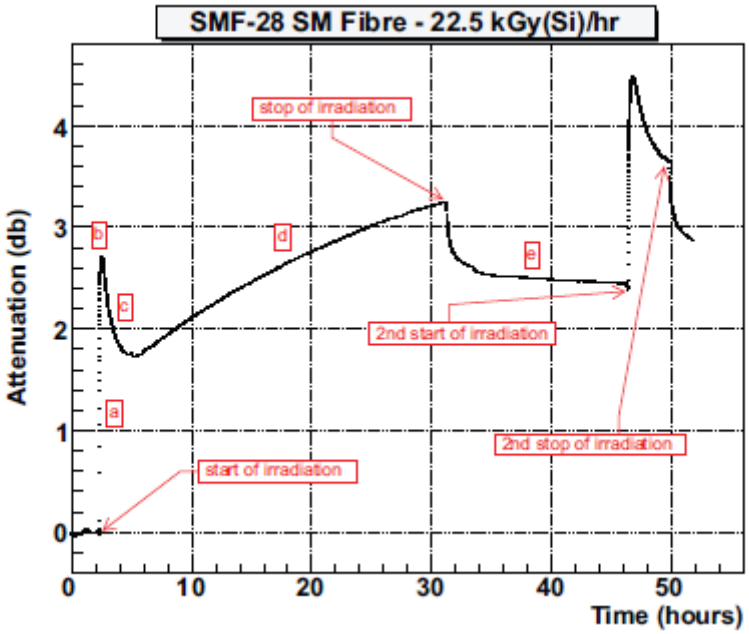

Figure 11 RIA for the Corning SMF28 fibre (SM) as a function of time during the exposure. The total dose corresponded to 650 kGy(Si).

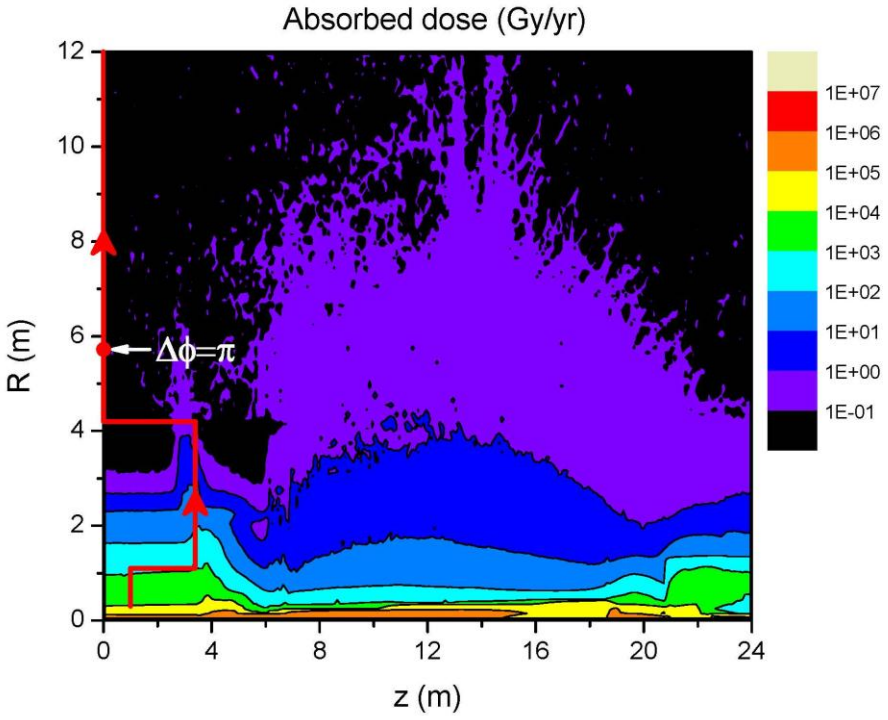

Figure 12 Fibre route (red line) superimposed on the ATLAS radiation dose map. The line includes the worst case scenario 180° routing around the voussoirs.

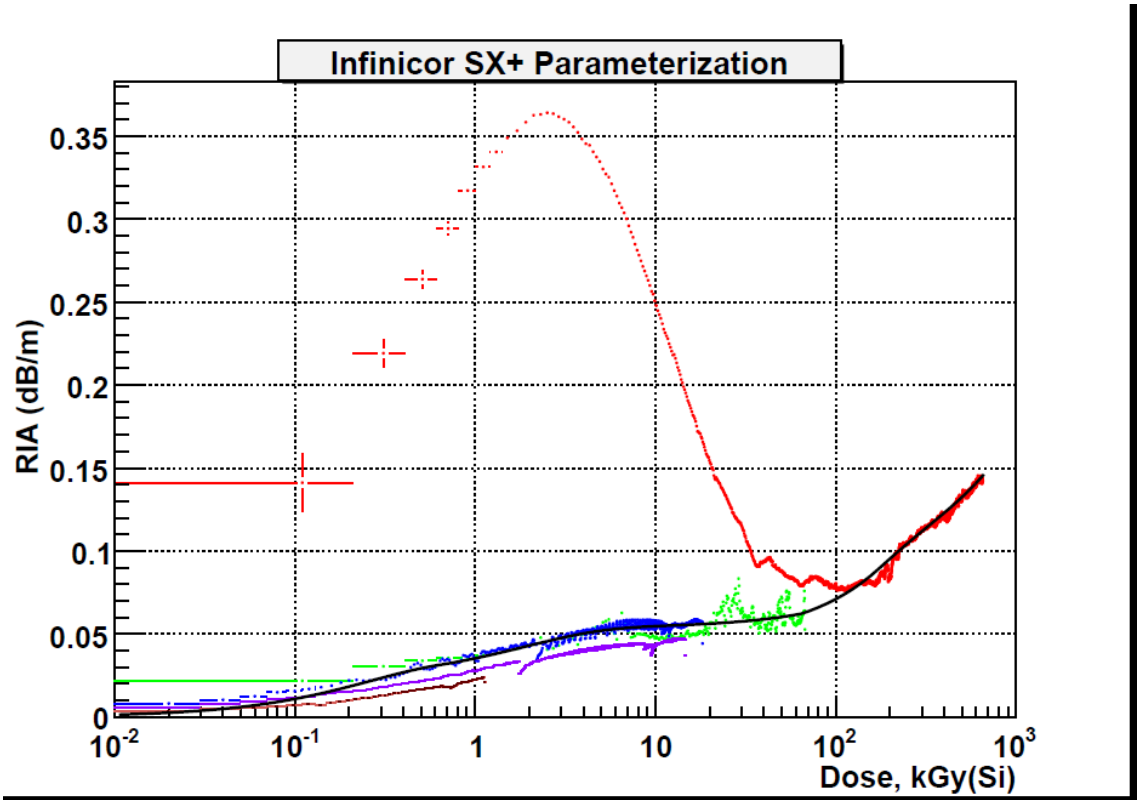

Figure 13 RIA versus dose for the SCK-CEN and BNL tests of the Infinicor SX+ fibre (MM). The dose rates for the red, green, blue, purple and brown data points were 22.5, 1.01, 0.48, 0.38 and 0.026 kGy(Si)/hour.

In addition to the RIA, the fibre reliability needs to be studied after the very high doses expected at HL-LHC. Fibre manufacturers have developed a methodology for determining the reliability of fibres based on measurements of pull tests. To study the mechanical quality of the fibre core, a pull test machine is used to measure the distribution of breaking stresses in a sample of fibres at a given pull speed. Although RIA is known to be sensitive only to ionizing dose as opposed to bulk damage, we do not know if this is also true for the mechanical properties of fibres. Therefore MM and SM fibre samples have been irradiated to a dose of 500 kGy(Si) at the ^{60}Co MegaCurie source in Taiwan and to a fluence of 10^{15} n_{1MeV_eq}/cm^2 at the TRIGA reactor in Ljubljana. The pull tests results from these samples will be compared with un-irradiated control samples to determine the effects of radiation on fibre reliability.

In addition to studying the mechanical strength of the core, it is also necessary to consider the quality of the acrylate buffer after radiation. The quality of the buffer is determined by micro-bending tests. In these tests the fibre attenuation is measured with an Optical Time Domain Reflectometer (OTDR) as the fibre is spooled onto a spool containing a special grade of sandpaper. The fibre is thus forced to make many micro-bends but if the quality of the buffer is good, these will be absorbed by the buffer, without putting any stress

on the core and hence not result in a large increase in attenuation. Samples of MM and SM fibre were irradiated to 500 kGy(Si) at the ^{60}CoMegaCurie source in Taiwan. As with the pull tests, control samples were also sent to Taiwan. The results of the micro-bending tests showed that the buffer quality improved slightly with radiation. This is thought to be due to the further polymerizing of the acrylalte by the radiation.

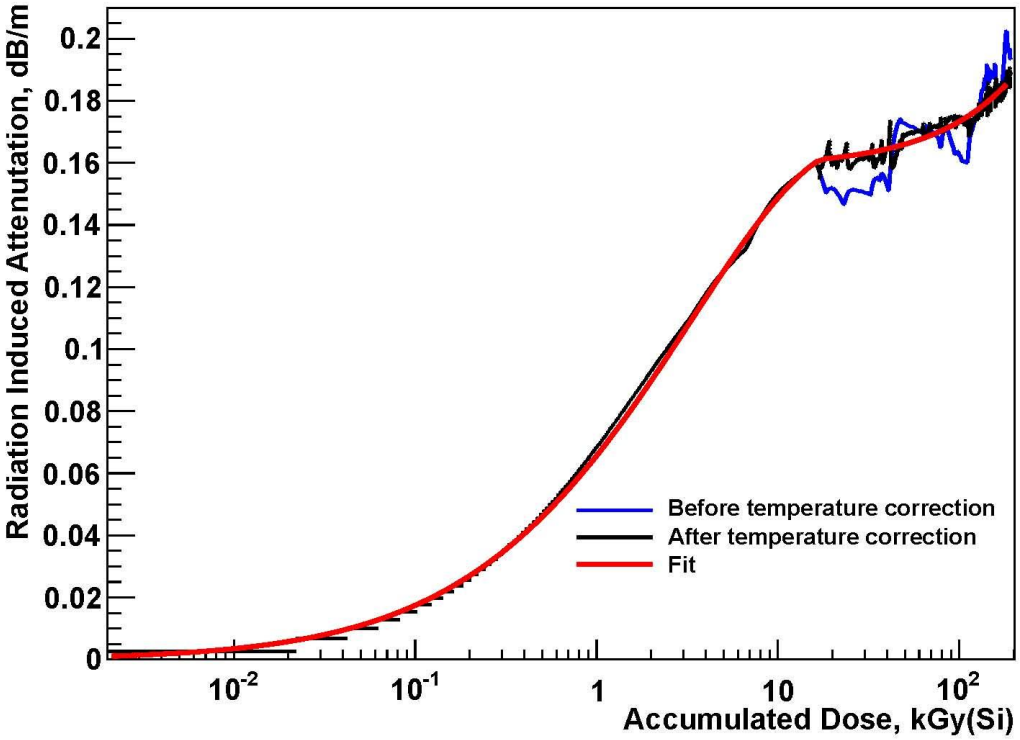

Figure 14 RIA versus dose for Corning SMF-28e SM fibre exposed at a temperature around T=-25°C. The data is shown before and after temperature corrections as well as an empirical fit.

4.2.2 Fibre Cable

For the long run of fibre from the outside of the ITK to USA15 the fibres will need to be in protective cables. For the current SCT and Pixel detectors, Fujikura and Ericsson cables are used which can contain up to 8 12-way fibre ribbons. A similar type of cable might be an option for the ITK, however many other types of high density cables are now available, some with even better packing density than those currently used. For example, Figure 15 shows a loose fibre cable which contains 288 fibres in a diameter of only 10.5 mm. The optimal choice of fibre cable will depend on routing considerations into the ITK which need to be studied.

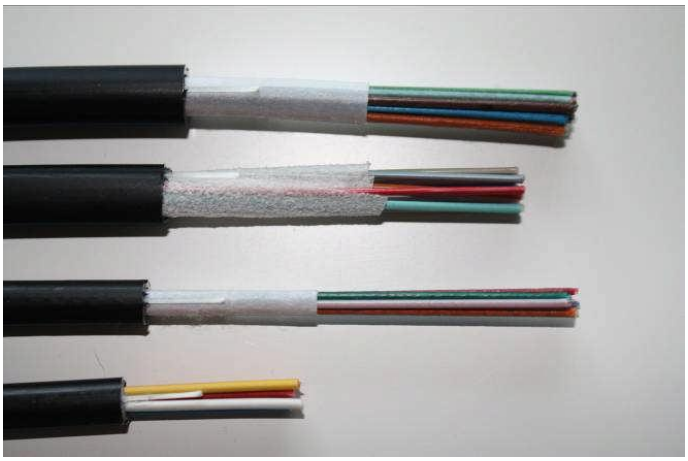

Figure 15 Loose tube fibre cable. Each of the coloured tubes can contain up to 12 individual fibres.

For the very high radiation levels at the HL-LHC, the radiation damage to the fibre cable must be evaluated. Some tests were performed by CMS up to LHC radiation levels but nothing is known about the effects of HL-LHC radiation levels. It is not known if ionizing dose or bulk damage effects are more important. Therefore these studies are being performed using 28 MeV protons from the Birmingham cyclotron. 11 cm lengths of the cable jacket and the CFRP strength members from the Ericsson and Fujikura cable were mounted on a scanning table. The table was scanned over the beam to achieve uniform irradiation up to an exposure of 10^{15} p/cm^2. This is an extreme value as it is higher than would be expected at any point along the cable in HL-LHC. Pull tests will be performed for irradiated and un-irradiated samples, when the levels of induced radioactivity have dropped to an acceptable level.

4.2.3 Fibre Connectors

The smallest form factor optical connectors available are LC single fibre connectors and MT connectors for ribbon fibres. The radiation hardness of these connectors was studied by measuring the insertion loss of these connectors, before and after being irradiated to a dose of 500 kGy(Si) ^{60}CoMegaCurie source in Taiwan. This actual dose expected will depend on the locations of the connectors inside the ITK but the dose used is certainly higher than that expected for any plausible location. The MT connectors used the MT/MPO adaptors to provide push-pull connectors. The summary of the insertion loss before and after radiation is given in Table 3. Even with the conservative dose used there is no evidence for any significant radiation damage for these connectors.

Fibre Connector	Mean Radiation induced insertion loss
LC	-0.11±0.05

MTP/MPO	0.17±0.13

Table 3 Insertion Loss measurements for fibre connectors. A positive number indicates radiation induced loss.

4.2.4 Optical Couplers

Optical couplers can be made from fused tapers, so that they only consist of fibres. The radiation tolerance of these type of connectors is then simply given by the radiation tolerance of the fibres. However these type of fibre couplers are too bulky for use in the ITK. For SM systems, very compact Planar Light Wave Couplers (PLC) are available. These use silica waveguides to split the input light into several output channels. Samples of 1*4 optical couplers were studied from three commercial suppliers as well as a prototype coupler using a glass substrate. The same methodology was used for these optical couplers as for the optical connectors. The results of the before and after irradiation comparison (also to a dose of 500 kGy(Si)) are summarized in Table 4. There is evidence for radiation damage to the glass based optical coupler but there is no evidence of any significant damage to the silica based optical couplers[15].

Device	Number Channels	Radiation Induced loss (dB)	
		Mean	Maximum
Browave	27	-0.23±0.04	0.29±0.10
Fibrenet 1	7	-0.59±0.14	-0.08±0.05
Fibrenet 2	4	1.08±0.09	1.16±0.08
Huihong	15	0.01±0.05	0.30±0.07

Table 4 Before and after radiation (500 kGy(Si)), insertion loss measurements for the optical couplers. The Fibrenet 2 device was based on a glass technology, all the others used silica. A postive number indicates radiation induced loss.

4.3 Backend Optoelctronics

The backend optoelectronics do not have any of the constraints of the on-detector components, therefore COTs are being evaluated to identify candidate devices that can satisfy the links budget. The first studies[16] were based on SFP+ transceivers and used to define the specifications for the link and to provide a set of reference components. Suitable components have been identified as illustrated in the “radar” plot in Figure 16.

While suitable SFP+ components are available, there is a clear interest in finding higher density components, so candidate array devices are being studied[16]. Several manufacturers now produce MT coupled VCSEL and *p-i-n* arrays for operation at 850 nm. Examples of candidate devices are shown in **Figure 17**. These devices are optical engines which mean they include laser drivers for the TXs and array TIA receivers for the Rxs. This allows for simple communication with standard digital I/O.

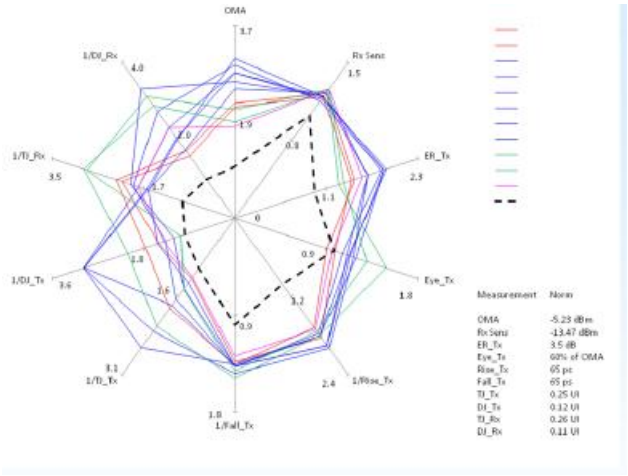

Figure 16 Radar plot for SFP+ candidate devices. OMA= optical modulation amplitude, Eye= vertical height of error free region at the centre of the eye diagram, ER=Extinction Ratio, Tr=rise time,Tf=fall time, Tj=total jitter, Dj=deterministic jitter. Values are normalised so that numbers above 1.0 exceed the specifications and numbers below 1.0 are outside specificaiton.

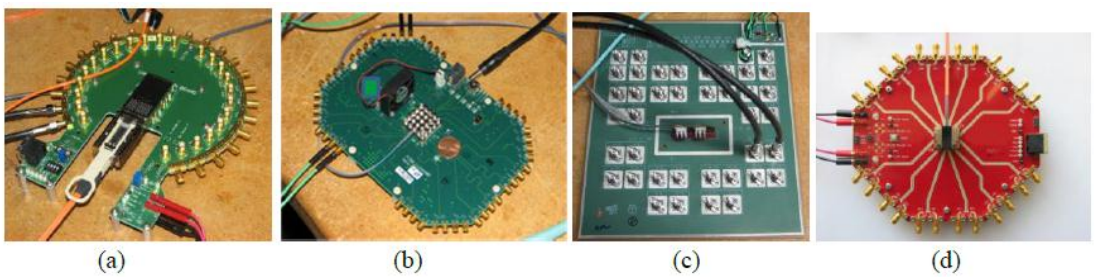

Figure 17 Some options for MM parallel optical links under study. (a) 12 channel TRx with 24 fibre MTP/MPO connector, (b) 12 channel TRx with a pig-tailed fibre ribbons and an

electrical connector, (c) shows a two 4 channel TRx devices with pig-tailed fibre ribbons (d) shows a 12 channel Tx also with a fibre ribbon connected by a Prizm optical connector. All the components are mounted on the manufacturer's evaluation PCBs.

Some of the devices being tested are still engineering samples, so the names of the manufacturers are confidential at this stage. The test results are shared with the manufacturers who can make further improvements before releasing commercial components. The test results show promising performance for these devices. The most difficult specification to achieve is that of the TX OMA because we have to allow for significant radiation damage to the *p-i-n* diode as well as RIA in the fibre (see Section 4.4). The OMA for three samples using VCSELs operating at 850 nm, is compared to the VL specification in Figure 18. Another critical specification is the jitter. The total jitter for the same devices is shown in Figure 19. We believe that suitable devices will be developed and if necessary device screening might be used to select devices with acceptable OMA. If it turns out to be impossible to obtain sufficiently high power TX arrays, then a backup solution would be to use high power single channel TXs and use the PLC optical couplers to broadcast the TTC data to several destinations.

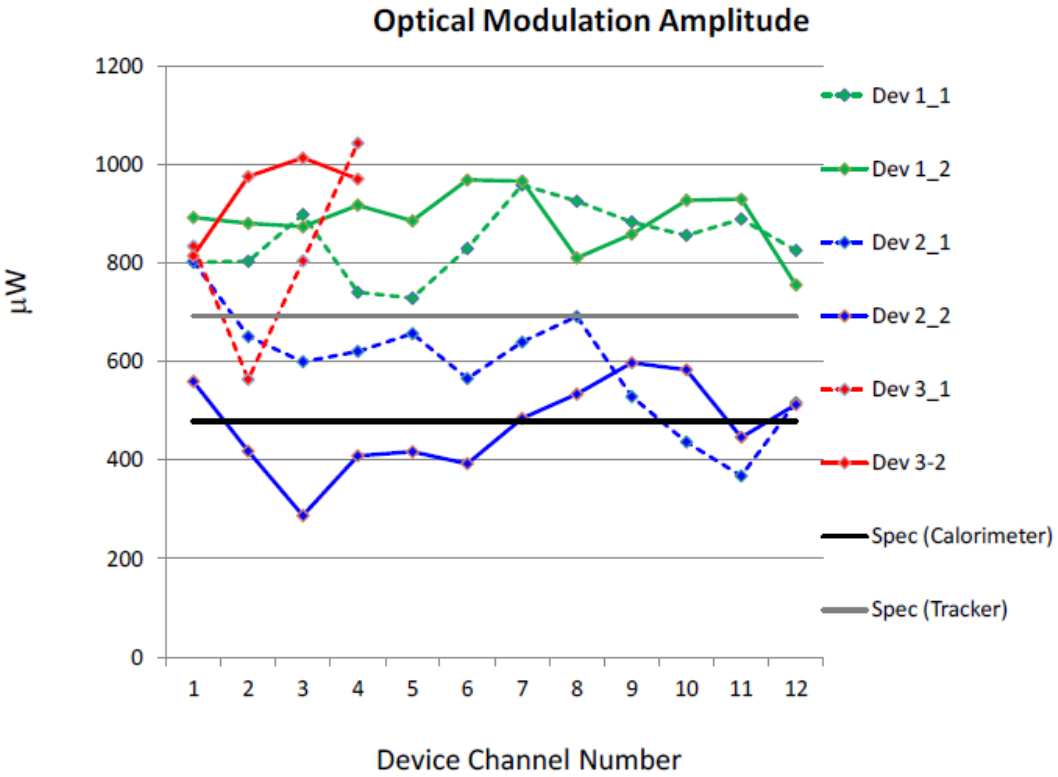

Figure 18 OMA versus channel number for 3 types of VCSEL MM parallel Tx devices. Data points above the thin horizontal line, represent channels that satisfy the VL specification.

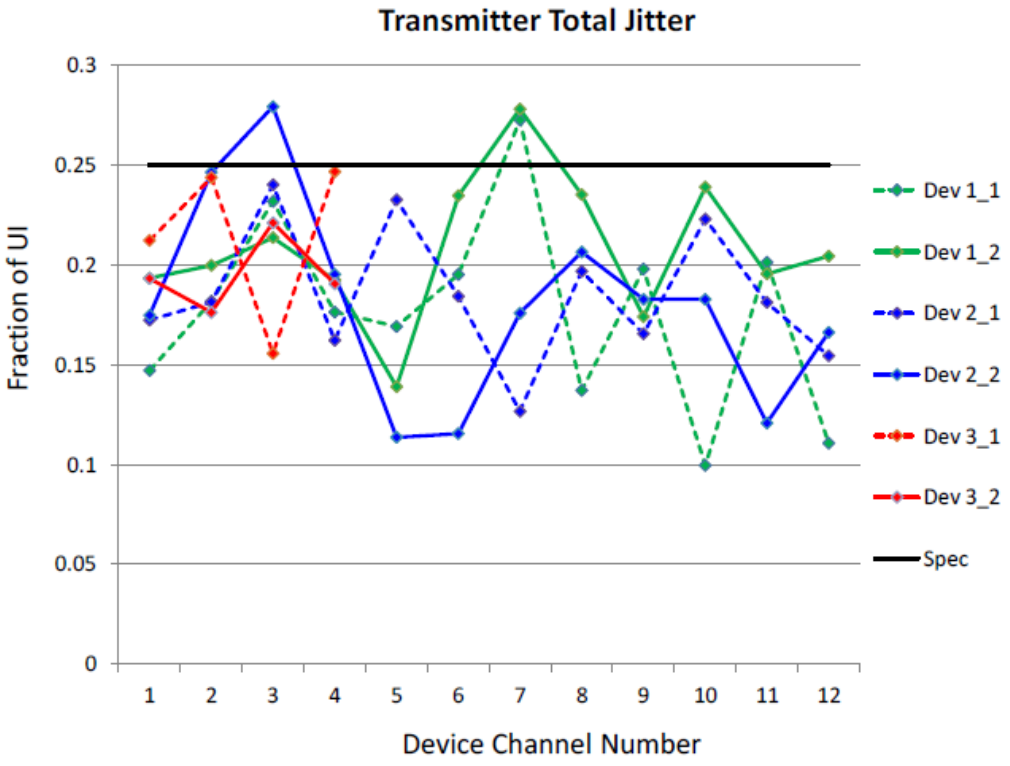

Figure 19 Total jitter versus channel number for the same devices as used for the data shown in Figure 18. UI=Universal Interval, i.e. the reciprocal of the bit rate. The total jitter specification is defined such that the contribution to the BER will be less than 10^{-12}.

For the *p-i-n* receivers the critical specifications are receiver sensitivity and jitter. The receiver sensitivity is measured by using optical attenuators to decrease the optical signal until the Bit Error Rate, BER=10^{-12}. The sensitivity versus channel number for some Rx devices operating at 850 nm are shown in Figure 20.

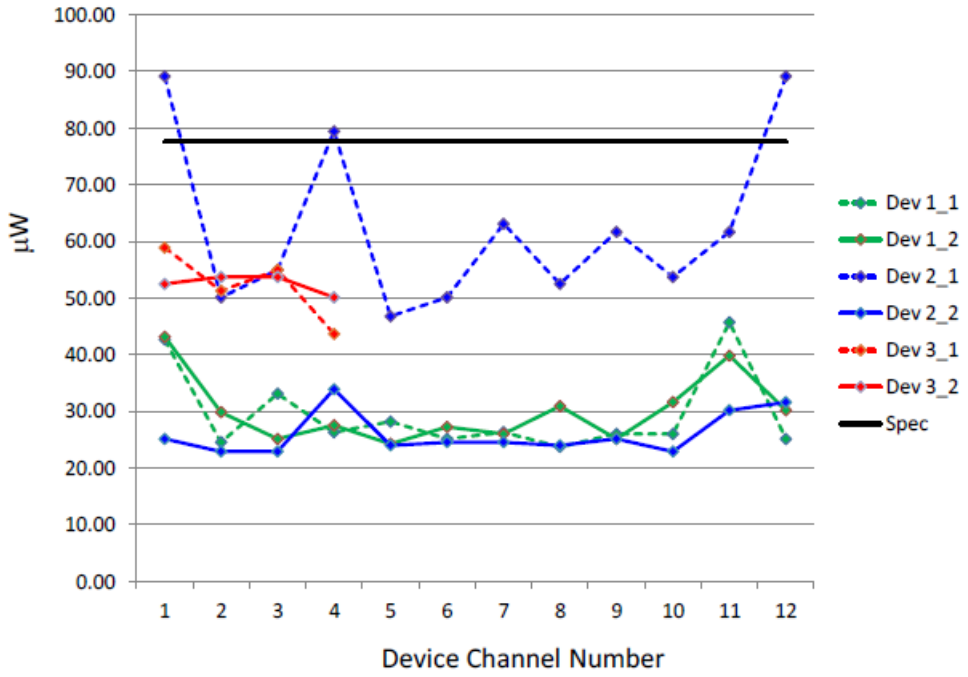

Figure 20 Sensitivity versus channel number for MM parallel optics Rx devices from three manufacturers. The solid line is the VL specification (values below this line represent channels satisfying the specification).

4.4 Link Budget

The link's power budget is based around the OMA available for the Tx devices and the sensitivity of the Rx devices. The power budget accounts for the losses in fibres and optical connectors. In addition link penalties are added in to take into account the effects of jitter in the Tx and Rx and dispersion in the fibre. The procedures used follow the industry standard (see http://www.ieee802.org/3/ae/public/adhoc/serial_pmd/documents/). This ensures that any pair of transmitters and receivers that satisfy the individual specifications will work correctly in an optical link. For the VL additional penalties are added to account for the expected effects of radiation damage on the on-detector Tx and Rx devices as well the optical fibre. A positive margin is achieved for all four flavours of the tracker version of the VL as shown in Table 5. The numbers shown all refer to worst case values, not typical. However the large radiation losses for the VRx will require larger OMA for the Tx than is currently standard (see section 4.3)

Table 5 VL power budget for MM (left) and SM (right) systems. VTx-Rx refers to "up-links" (data) and Tx-VRx to "down links" (TTC). If error corrections is used the margin is increased by 2-3 dB. The optical power is specified in dBm which measures the signal relative to 1 mW, in dB.

Specification	MM_VTx_Rx	MM_TX-VRx	SM_VTx_Rx	SM_TX-VRx
Minimum Tx OMA (dBm)	-5.2	-1.6	-5.2	-3.6

Maximum Rx sensitivity (dBm)	-11.1	-13.1	-12.6	-15.4
Power budget (dB)	5.9	11.5	7.4	11.8
Fibre attenuation	0.6	0.6	0.1	0.1
Insertion loss (3 break points)	1.5	1.6	2.0	2.0
Link penalties	1.0	1.0	1.5	1.5
Tx radiation penalty	0	-	0	-
Rx radiation penalty	-	5.4	-	
Fibre radiation penalty	1.0	1.0	1.0	1.0
Margin	1.8	2.0	2.8	1.8

4.5 Links Electrical Power Budget

It is important to minimize the electrical power for the on-detector components. The electrical power budget of the VTRx is given in Table 6.

Table 6 Electrical power consumption for the components of one VTRx. The GBTx is included for completeness. The power consumption for the GBLD includes the power dissipation in the lasers. The minimum power for GBLD refers to the case of a single channel, operating at minimum bias and modulation current and the maximum power refers to the case of two channels being operated at maximum bias and modulation currents. The maximum power therefore covers the worst case for the power using EELs after radiation damage.

Item	Minimum Power (mW)	Maximum Power (mW)
GBTx		1800
GBLD	217	735
GBTIA		120

4.6 Links for Pixel System

Due to the high radiation levels as well as the space constraints inside the Pixel detector volume, the optical components will be placed at a larger radius possibly outside the ITk volume. Therefore an electrical link between the detector electronics and the optoboard, holding the optical components needs to be installed over a length of 4-6m.

The architecture of the transmission scheme is shown in Figure 21. The modules of a half stave will be connected electrically to the end of stave card (EOS). The optical components on the optoboards are then located around 4-6m away from the EOS. To link the EOS with the optoboard a GBT chipset is foreseen on both ends. Line drivers will transmit the signals to and from the detector between these two boards.

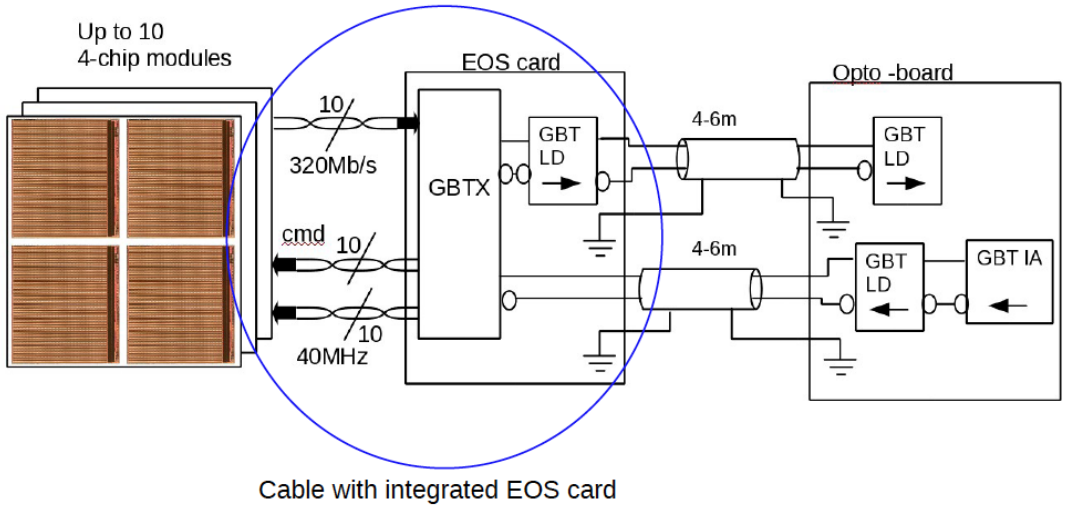

Figure 21: Proposed readout architecture for multichip Pixel modules

The outer part of the Pixel detector for ITK will be constructed of multichip modules (4 chips per module). A possible readout chip is the FE-I4 chip which has been developed for the IBL upgrade of the old Pixel detector. The innermost part will most likely be assembled from single or double chip modules, for which the chip itself has not yet been decided.

The output data rate of a Pixel module assembled from 4 FE-I4 readout chips is foreseen to be 320 Mbit/s. Up to 10 of these modules will be combined into one optical transmission line. Equivalently the innermost part is assumed to have the same bandwidth for fewer chips.

Using the Versatile Link architecture, the TTC link consists of an optical receiver (Rx) *p-i-n* diode (included in the VTRx) coupled to a GBT TIA (Trans Impedance Amplifier). The electrical signals are then driven to the EOS located inside the detector volume using a GBT LD. The GBT chipset on the EOS needs to decode the received signal into clock and data for the connected modules into separate lines or a bus.

The opposite direction (Tx) is handled the same way. The data from the up to 10 modules are combined into one fast data link (GBT serializer) and then driven by GBT LD to the optoboard on which the data then is driven to a laser using another GBT LD. The laser is again included in the VTRx.

It is necessary, that the electrical link between the EOS and optoboard is capable of transmitting high-speed data (3.2 Gbit/s). Micro coax cables are an option here. Cable impedance is a key issue here and needs careful testing and qualification.

A test of this architecture is planned in the near future. The GBT v4 chipset can be used to implement a data transmission path between the now available FE-I4 chips and an optoboard placeholder built from a GBT chipset.

With this setup it is required to qualify the type of cables needed for the linking as well as testing the bandwidth capabilities, signal quality, link performance, stability, and further items of the whole transmission link. First optical components will be used to extend the link by the optical path and do a full link study.

4.7 New GBTx

After submission of the current GBTx in August 2012, there is a plan to work on a new design called lpGBTx in 65 nm technology. The aim is to decrease the power by about a factor of ¼ and double the bandwidth to give 9.6 Gbits/s bit rate and a user bandwidth of 6.4 Gbits/s. The baseline solution for the links assumes that the lpGBTx will be available. A backup solution with the current version of GBTx would need to drop the Forward Error Correction (FEC) for the data links.

4.8 Numerology and Costings

Using the LoI layout and assuming that no redundancy is used the number of links for the ITK can be evaluated. The current estimates are based on the assumption that the RoI track trigger is used for the strip detector, so that the bandwidth is sufficient for rates at L0(L1) of 500 (200) kHz. However the current design of the pixel chip does not allow for the reduced readout at L0, therefore the bandwidth for the pixels is based on full readout at the L0 rate of 500 kHz. The number of links in the different subsystems is given in Table 7. Note that each link here refers to a pair of data and TTC links.

Table 7 Number of optical links for the ITK LoI layout.

Sub-system	Number of links
Pixel barrel	812
Pixel disks	288
Strip barrel	1200
Strip End Caps	896

Total	**3196**

The estimated total cost is in the range 1.2 to 1.9 MCHF. Accurate costings will only be available once the particular variant of the VL for the ITK has been selected. If the number of links need to be reduced for cost or material budget reasons, the options that should be considered are:

- Decrease the bandwidth for the pixels by implementing an RoI track trigger readout, so that readout at L0 would be reduced from 500 kHz to 200 kHz.
- Turn of Forward Error Correction (FEC) in the data links to increase the user bandwidth from 6.4 Gbits/s to 8.96 Gbits/s.
- Readout both sides of petals through one EoS card and one VL link.

5. Summary and Outlook

The feasibility of the VL for use in the ITK at HL-LHC has been established and can therefore provide a baseline solution for the optical links for the ITK. However, further developments in the available technologies, might result in improvements to the system. In the context of the VL R&D work remains to be done before production:

- For the on-detector VTx and VRx, the plastic parts needs to be optimized and a scheme for mass production developed.
- For the passive components, the study of the reliability of the fibre and cable after HL-LHC radiation needs to be completed. A suitable cable has to be selected based on detailed considerations of the fibre routing in ATLAS;
- For the backend Txs more work is required to identify suppliers capable of meeting the higher OMA specifications of the VL.
- High speed (9.6 Gbits/s) short distance electrical links need to be demonstrated for the pixel readout.

In addition the new lpGBTx will need to be designed and demonstrated to run at the required speed. The timescale for the completion of the R&D associated with the on-detector components is of the order of one year but more time is available for the off-detector components.

In the production phase as well as performing QA on all components, it will be necessary to perform radiation hardness tests on sample VTRx, optical fibres and connectors. The fibres will be produced from a few performs, so one sample from each perform will be studied.

High speed electrical links will need to be developed to transfer the data from the pixel detector to a location at larger radius, where the optoelectronics would be located. There is on-going R&D on the low mass, high speed electrical cables.

6. Acknowledgements

I wish to thank my colleagues, Francois Vasey and Jan Troska from the Versatile Link project for reading draft versions of this document and making corrections and useful suggestions.

References

[1] VCSEL status and development of robust arrays,2012 *JINST* **7** C01098 **doi:10.1088/1748-0221/7/01/C01098**.

[2] L. Amaral et al., The Versatile Link, a common project for Super-LHC, JINST 2009 4 P12003, **doi:10.1088/1748-0221/4/12/P12003**

[3] GBTx, https://espace.cern.ch/GBT-Project/GBTX/Specifications/Forms/AllItems.aspx.

[4] H. Desmond, Data scrambling report, https://espace.cern.ch/project-atlas-stripsreadout/Shared%20Documents/Data%20format/Scrambler_Report.pdf

[5] GBLD, https://espace.cern.ch/GBT-Project/GBLD/_layouts/viewlsts.aspx?BaseType=1.

[6] C. Garcia Argos et al, Measurement of the potential electromagnetic interaction of the Versatile Link with the Strips Upgrade Stavelet, ATL-COM-UPGRADE-2012-014, https://cdsweb.cern.ch/record/1458065/files/ATL-COM-UPGRADE-2012-014.pdf

[7] GBT-TIA, https://espace.cern.ch/GBT-Project/GBTIA/default.aspx.

[8] C Soós et al., Versatile Transceiver development status, 2012 *JINST* **7** C01094 **doi:10.1088/1748-0221/7/01/C01094**.

[9] J. Troska et al., Radiation damage studies of lasers and photodiodes for use in multi-Gb/s optical data links, proceedings NSREC 2011, Las Vagas, July 25-29 2011.

[10] F. Vasey et al., The Versatile Link common project: feasibility report, 2012 *JINST* **7** C01075, **doi:10.1088/1748-0221/7/01/C01075.**

[11] B. Arvidson et al., Radiation resistance of specific optical fibres exposed to 650 kGy(Si) of ionizing radiation, JINST_002P_0609,doi: 10.1088/1748-0221/4/07/P07010.

[12] B.T. Huffman et al., The radiation hardness of specific multi-mode and single-mode optical fibres at -25°C beyond a full SLHC dose, to a dose of 500 kGy(Si), 2010 *JINST* **5** C11023 **doi:10.1088/1748-0221/5/11/C11023.**

[13] D. Hall et al., radiation induced attenuation of optical fibres below −20°C exposed to lifetime HL-LHC doses at a dose rate of 700 Gy(Si)/hr, 20012 *JINST* **7** C01047 **doi:10.1088/1748-0221/7/01/C01047.**

[14] D. Hall et al., The radiation tolerance of MTP and LC optical fibre connectors to 500 kGy(Si) of gamma radiation, 2012_JINST_7_P04014, **http://dx.doi.org/10.1088/1748-0221/7/04/P04014.**

[15] N.C Ryder et al., The Radiation hardness and temperature stability of Planar Light-Wave Circuits for the High Luminosity LHC, 2010 *JINST* **5** C11023 **doi:10.1088/1748-0221/5/11/C11023.**

[16] J Chramowicz et al., Evaluation of emerging parallel optical link technology for High Energy Physics, 2012 *JINST* **7** C01007 **doi:10.1088/1748-0221/7/01/C01007.**

[17] The radiation induced attenuation of optical fibres below −20°C exposed to lifetime HL-LHC doses at a dose rate of 700 Gy(Si)/hr, 20012 *JINST* **7** C01047 **doi:10.1088/1748-0221/7/01/C01047**